Competing length scales in anharmonic lattices: Domains, stripes, and discommensurations

A. Bussmann-Holder
Max-Planck-Institut für Festkörperforschung, Heisenbergstrasse, 70569 Stuttgart, Germany

A. R. Bishop
Los Alamos National Laboratory, Theoretical Division, Los Alamos, New Mexico 87545

(Received 6 December 1996; revised manuscript received 28 April 1997)

A two-dimensional anharmonic electron-lattice interaction model with higher-order density-density-multiphonon interactions is solved exactly for arbitrary reciprocal-lattice vector q in the ionic limit as a model of a transition-metal oxide. Combining the harmonic and higher-order electron-phonon interaction terms into an effective coupling yields a strong q dependence of this coupling which changes sign when an on-site double-well potential occurs. Depending on the depth of this double-well potential various mesoscale structural and polarization patterns are found: stripes and domains, as well as incommensurate structural modulations. The results are related to experimental data for high-temperature superconductors, colossal magnetoresistance, and ferroelectric transition-metal perovskites, which probe local structural effects [S0163-1829(97)03334-1]

In the last few years a variety of experimental techniques have been developed which are able to test local structural effects in solids. These techniques work on a different time scale than conventional scattering experiments and superficially their results seem, partially, to be conflicting with results obtained from conventional structural methods. From extended x-ray-absorption fine structure, pair-distribution function, nuclear magnetic resonance, etc., it is, for instance, concluded, that the local structure of high-T_c superconductors[1] and oxide ferroelectrics[2] deviates substantially from the average structure as, e.g., obtained from x-ray or neutron crystallography. As the former experiments are based on a much faster time scale than the latter, the results are in fact not in conflict but rather show that the various collective particle dynamics are governed by different time[3,4] and length scales. In a recent molecular-dynamics simulation of a model ferroelectric[5] it has been shown that the coexistence of these various time (and associated length) scales gives rise to a central peak in addition to mode softening, and a coexistence regime of order-disorder and displacive behavior.

In the following we study a two-dimensional nonlinear electron-ion interaction Hamiltonian which is not only anharmonic in the ionic displacement field but also contains, in addition to linear electron-phonon coupling, terms higher order in electron-density multiphonon interactions.[6] The Hamiltonian is equivalent to the nonlinear shell model[7] and represents the highly polarizable nature (through spin-charge-lattice coupling) of transition-metal oxides with strong p-d hybridization.

These systems are known to be very anharmonic and to show a strong tendency towards charge transfer and disproportionation. Also is has been shown experimentally that specifically the oxygen ions show a tendency toward local structural displacements which deviate substantially from their ideal crystallographic position.[1] Our Hamiltonian for a square face-centered-cubic diatomic lattice reads

$$H = H_{\text{latt}} + H_{\text{el}} + H_{\text{el-latt}},$$

$$H_{\text{latt}} = \sum_{\substack{i=1,2 \\ l,l',l'',l'''}} \left[\frac{(P_l^{(i)})^2}{2} + \frac{(\omega_l^{(i)})^2}{2} (Q_i^{(i)})^2 + \frac{g_4}{4} Q^{(1)}{}_l Q^{(1)}{}_{l'} Q^{(1)}{}_{l''} Q^{(1)}{}_{l'''} \right] \tag{1}$$

$$- 1/2 \sum_{ll'} V_{ll'}{}^{(1)} Q_l{}^{(1)} Q_{l'}{}^{(l)}, \tag{1a}$$

$$H_{\text{el}} = \sum_{k,k'} (\varepsilon_k n_k + V_{kk'} n_k n_{k'}), \tag{1b}$$

$$H_{\text{el-latt}} = \frac{1}{\sqrt{N}} \sum_{\substack{i=1,2 \\ q}} g_2{}^{(i)}(q) n_q \sqrt{\frac{2M_i \omega_q{}^{(i)}}{\hbar}} Q^{(i)}{}_{-q} + \frac{1}{\sqrt{N}} \sum_{q,q',q''} g_4(q) n_q \sqrt{\frac{2M_1 \omega_q{}^{(1)}}{\hbar}} Q^{(1)}{}_{-q} \times \left\{ n_{q'} Q_{-q'}{}^{(1)} \sqrt{\frac{2M_1 \omega_{q'}{}^{(1)}}{\hbar}} + Q_{-q''}{}^{(1)} Q_{-q'''}{}^{(1)} \frac{2M_1}{\hbar} \omega_{q''}{}^{(1)} \omega_{q'''}{}^{(1)} \right\}. \tag{1c}$$

Here, $P^{(i)}$, $Q^{(i)}$ are momentum and conjugate displacement coordinates of ion i with mass m_i; $\omega^{(i)}$ are the corresponding harmonic mode frequencies, where $\omega^{(1)}$ is explicitly allowed to become unstable [i.e., $(\omega^{(1)})^2 \leqslant 0$]; g_4 is the on-site anharmonicity of ion 1 which is assumed to represent the oxygen ion. $V_{ll'}{}^{(i)}$ is the nearest-neighbor interaction between ions M_i [l corresponds to the reciprocal-lattice vector $q=(q_x,q_y)$]. ε_k is the band energy, which is in the following assumed to be negligible, i.e., we are dealing with an

ionic system. This obviously corresponds to commensurate charges. The Coulomb repulsion is given by $V_{kk'}$ and $n_k = c^+{}_k c_k$. The interaction Hamiltonian contains the usual harmonic couplings $g_2^{(i)}$, where $g_2^{(1)}$ acts as on-site and $g_2^{(2)}$ as intersite, and in addition higher-order density-density-multiphonon interactions proportional to g_4, which act at the oxygen ion lattice site only. The total electron-lattice interaction, as given by the last equation, defines a new renormalized interaction which, as will be shown below, is significantly modified through the higher-order terms as compared to the purely harmonic coupling case. We will concentrate mainly on this term, which will be shown to control local structural effects. If the harmonic couplings are sufficiently strong, polaron formation can take place. This, of course, might become virtual only, if the terms proportional to g_4 are repulsive, but on the other hand, it is also possible that for weak $g_2^{(i)}$ a polaronic state can exist if g_4 acts in the same direction. A lattice instability may arise from different sources; namely (i) one of the harmonic mode frequencies may become imaginary; (ii) the harmonic electron-lattice coupling can compensate a stable harmonic mode frequency and drive it to zero; (iii) the higher-order density-phonon terms can destabilize the lattice even if the harmonic interaction is small. A Jahn-Teller instability may arise if the band energy is replaced by exchange coupling.

In the following we proceed with the diagonalization scheme proposed in Refs. 8 and 9 and concentrate on the lattice Hamiltonian only — in order to evaluate the possibility of electron-phonon interaction induced stripe, domain, or incommensurate ground states, and transitions between them. The renormalized electronic Hamiltonian will be discussed elsewhere. However, we note here that it can be shown that superconductivity can arise through two coupled channels, where one is attributed to an electron-phonon driven instability of the Fermi liquid, while the other one arises from a polaronic band which becomes virtual due to the multiphonon contributions.

In order to solve the above system we make two approximations, the first one, i.e., $\varepsilon_k = 0$ has already been mentioned and corresponds to the ionic limit and commensurate charges. The second approximation is $l = l' + l'' + l'''$ and $\omega_{q,l} = \omega_{q',l'} + \omega_{q'',l''} + \omega_{q''',l'''}$, i.e., Umklapp processes are neglected and the phonon decay is restricted to the indicated processes. This allows us to Fourier transform the equations of motion in $Q^{(i)}$, but still explicitly includes the cubic terms appearing in $Q^{(i)}$. This procedure is a clear improvement compared to mean-field treatments, where pair product operators in the phonon displacement fields are used in order to evaluate the dynamics.[8,10] Most importantly, mean-field approximations yield a q-independent effective coupling, whereas in the present case the q dependence of the effective electron-ion coupling can be explicitly incorporated. The Coulomb repulsion in the electronic Hamiltonian can be absorbed in the density-density multiphonon interaction, which (when it is attractive) may strongly screen the long-range repulsion.

The equations of motion are obtained by conventional Fourier transformation, i.e., $Q_{lq}{}^{(i)} = -[[Q_q{}^{(i)}, H], H]$, where, as already outlined above, the approximation of replacing pair product operators by their expectation values is not made. This yields a set of nonlinearly coupled equations of motion:

$$-M_1\omega^2 Q_q{}^{(1)} = \Bigg\{ -V_{qq'}{}^{(1)} - (\omega_q{}^{(1)})^2 - g_4 (Q_q{}^{(1)})^2 - \varepsilon_F \cdot (\omega_q{}^{(1)})^2 \lambda_2^{(1)} J \Bigg[1 + \varepsilon_F (\omega_{q'}{}^{(1)})^2 \frac{\lambda^4}{\lambda_2{}^{(1)}} \times J + \frac{\lambda^4}{\lambda_2{}^{(1)}} (Q_{q''}{}^{(1)})^2 (\omega_{q''}{}^{(1)})^4 \Bigg] \Bigg\} Q_q{}^{(1)}, \tag{2a}$$

$$-M_2\omega^2 Q_q{}^{(2)} = -\{(\omega_q{}^{(2)})^2 + \varepsilon_F (\omega_q{}^{(2)})^2 \lambda_2{}^{(2)} J\} Q_q{}^{(2)}, \tag{2b}$$

$$[(\omega_q{}^{(1)})^2 + g_4 (Q_q{}^{(1)})^2] Q_q^{(1)} = -Q_q{}^{(1)} \varepsilon_F (\omega_q{}^{(1)})^2 \lambda_2{}^{(1)} J \Bigg\{ 1 + (\omega_{q'}{}^{(1)})^2 \varepsilon_F \frac{\lambda_4}{\lambda_2{}^{(1)}} J + \frac{\lambda_4}{\lambda_2{}^{(1)}} (\omega_{q''}{}^{(1)})^4 Q_{q''}{}^{(1)})^2 \Bigg\} + Q_q{}^{(2)} \varepsilon_F (\omega_q{}^{(2)})^2 \lambda_2{}^{(2)} J. \tag{2c}$$

Equation (2c) yields the coupling between the two sublattices which is given through the interaction with the electrons only. The λ are

$$\lambda = \frac{2g^2}{2\hbar\pi\varepsilon_F\omega} \tag{3a}$$

and

$$J = \int_0^{2\pi/a} \frac{1}{E_k} \tanh \frac{E_k}{2kT} dk, \tag{3b}$$

$$E^2{}_k = \pi\varepsilon_F \Bigg\{ \sqrt{\lambda_2}{}^{(2)} \omega_q{}^{(2)} Q_q{}^{(2)} + \sqrt{\lambda_2}{}^{(1)} \omega_q{}^{(1)} Q_q{}^{(1)} \times \Bigg[1 + \sqrt{\frac{\lambda_4}{\lambda_2{}^{(1)}}} [\omega_{q'}{}^{(1)} Q_{q'}{}^{(1)} \varepsilon_F + (\omega_{q''}{}^{(1)} Q_{q''}{}^{(1)})^2] \Bigg] \Bigg\}^2. \tag{3c}$$

Without the neglect of the band energy ε_k, Eq. (3c) would correspond to a gap equation for the electronic energies. Note that this gap experiences dramatic modifications from the higher-order terms as compared to conventional electron-lattice couplings. It is especially worth noting that a strong q

TABLE I. Parameters used in the calculations.

ω_1^2(THz^2)	ω_2^2(THz^2)	$\lambda_2^{(2)}$	λ_4
3.28	19.74	14.41	2.9

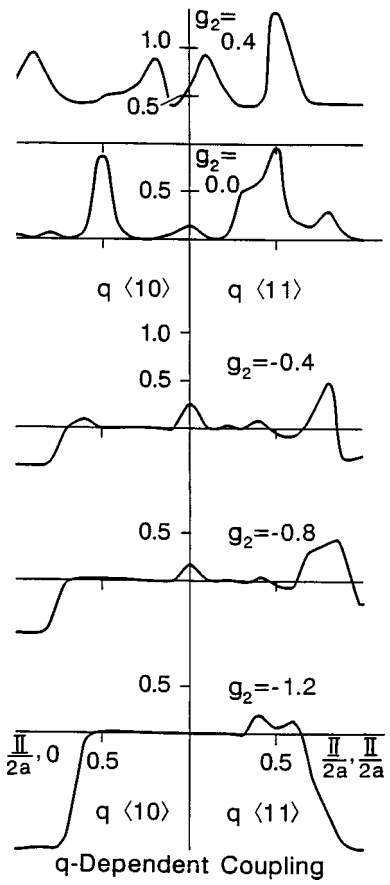

FIG. 1. q-dependent effective electron-phonon coupling along $\langle 11\rangle$, $\langle 10\rangle$ with $\lambda_2^{(1)}$ (from top to bottom): 0.4, 0.0, -0.4, -0.8, -1.2.

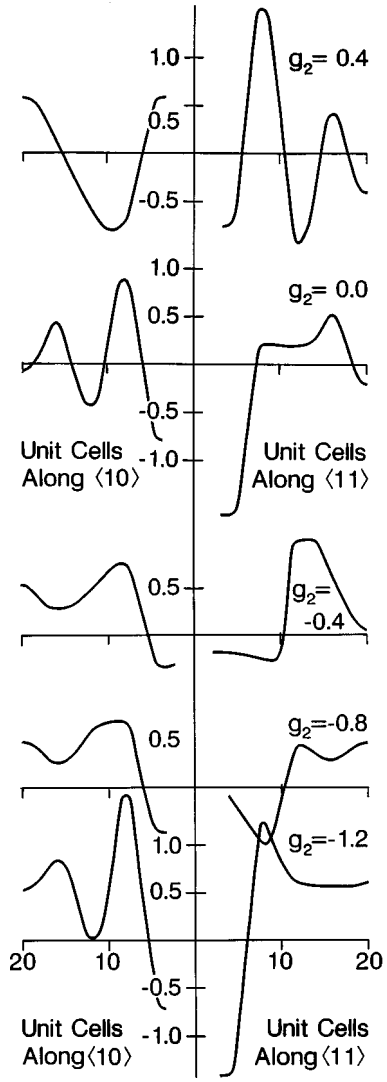

FIG. 2. Real-space effective electron-phonon coupling along $\langle 11\rangle$, $\langle 10\rangle$ with $\lambda_2^{(1)}$ (from top to bottom): 0.4, 0.0, -0.4, -0.8, -1.2.

dependence and consequently large anisotropy will result. Also doping will be affected strongly through these renormalizations. The consequences of this effect will be discussed elsewhere. In the zero-temperature limit, to which we restrict the present discussion, the integral can be solved analytically. Instead of performing the integration, we transform Eqs. (3) to the corresponding summation over k as we are interested in the q-dependent effects on the effective electron-phonon coupling, local dipole moments, and possible local structural instabilities. Inserting Eq. (3) into the equations of motion gives a set of nonlinearly coupled equations in $Q_q^{(i)}$. We solve this set numerically: Starting from trial frequencies ω to obtain $Q_q^{(i)}$, we reinsert these in the equations of motion to obtain the new frequencies and iterate until covergence is achieved. Typically, the convergence is very slow, indicating metastability and complex spatial structure. An effective q-dependent electron-phonon coupling is obtained by summing the couplings appearing in Eq. (3c). The parameters of the systems are then the harmonic lattice frequencies, the linear coupling constants, and the higher-order coupling (see Table I). We keep all quantities constant except for $\lambda_2^{(1)}$. $\lambda_2^{(1)}$ has the character of an effective temperature as, in the attractive case, it may destabilize the harmonic mode frequencies $\omega_q^{(i)}$ thus inducing double-well structures in the renormalized on-site potential energy.

In Fig. 1 the results for the effective q-dependent coupling are given. The top panel is the case where the coupling $\lambda_2^{(1)}$ is repulsive which yields a repulsive coupling in both directions $\langle 11\rangle$ and $\langle 10\rangle$. Even though the lattice is stable for all q values, large fluctuations in the coupling are observed in both directions which is already an indication of incipient local structural distortions. If the harmonic coupling is zero (second case from top in Fig. 1) instabilities are observed, because of broad regions in the q space where the coupling is close to zero. For $\lambda_2^{(1)}<0$ (third–fifth cases in Fig. 1) a sign reversal is obtained at finite q, whereas at $q=0$ the effective coupling is still repulsive. This indicates that the lattice undergoes a structural (superlattice) distortion on specific length scales. To clarify this finding in more detail we have transformed the effective coupling to real space (Fig. 2). The repulsive case shows large fluctuations of the effective coupling of the order of four lattice constants along the $\langle 11\rangle$ direction and ten lattice constants along $\langle 10\rangle$. The $\lambda_2^{(1)}=0$ limit shows the onset of a stable lattice along $\langle 11\rangle$ on the scale of ten lattice constants and fluctuating regimes exist along $\langle 10\rangle$ with a period of four lattice constants. This case clearly indicates the formation of stripes along $\langle 10\rangle$ which

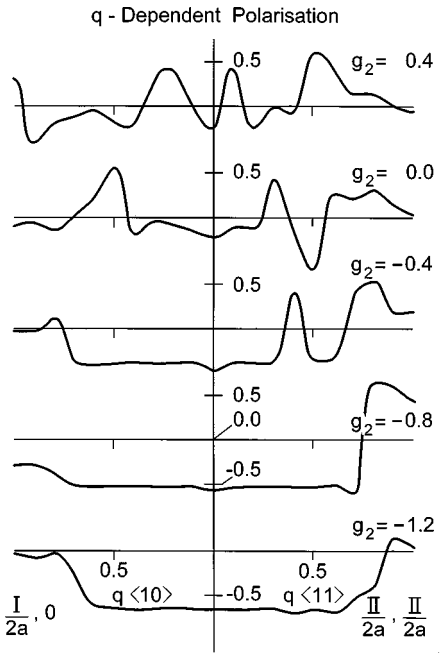

FIG. 3. q-dependent polarization along $\langle 11\rangle$, $\langle 10\rangle$ with $\lambda_2{}^{(1)}$ (from top to bottom): 0.4, 0.0, −0.4, −0.8, −1.2.

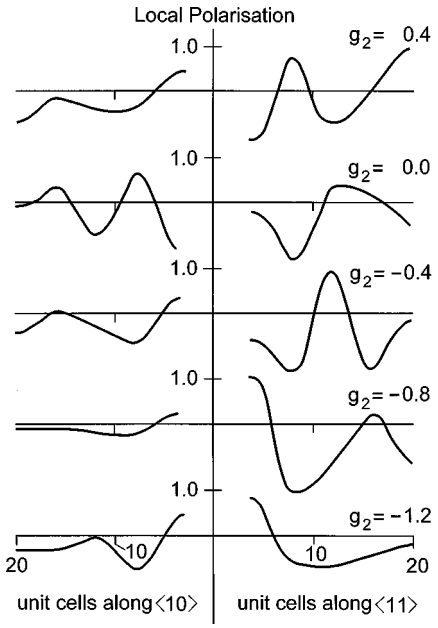

FIG. 4. Real-space polarization along $\langle 11\rangle$, $\langle 10\rangle$ with $\lambda_2{}^{(1)}$ (from top to bottom): 0.4, 0.0, −0.4, −0.8, −1.2.

are not present along $\langle 11\rangle$. In the $\lambda_2{}^{(1)}<0$ limit $[\lambda_2{}^{(1)}=-0.4]$ which is of greatest interest here, stripe formation is observed along $\langle 11\rangle$ and fluctuating regimes along $\langle 10\rangle$. This case clearly will give rise to a ''tweedlike''[11] dynamical incommensurate superstructure. Decreasing $\lambda_2^{(1)}$ further (second case from bottom in Fig. 2) shows the onset of stabilization of the structure along both directions beyond a scale of 10 (along $\langle 11\rangle$) and 5 (along $\langle 10\rangle$) lattice constants. Here stripe formation should occur which will be evidenced more clearly by investigating the local displacement pattern. For deep local double-well potentials (last case in Fig. 2) the size of striped areas along $\langle 11\rangle$ increases together with the formation of a superstructure along $\langle 10\rangle$. This case indicates the onset of fluctuating domains competing with stripes, which corresponds to a tweedlike pattern.

The same conclusions can be drawn from investigating the q dependences of the displacement fields $Q_q^{(1)}$ and $Q_q^{(2)}$ with respect to each other. If the two ions are assumed to have opposite charges, their relative displacement defines a q-dependent polarization wave. This is shown in Fig. 3 for the same set of $\lambda_2{}^{(1)}$ values as before. In the repulsive and $\lambda_2^{(1)}=0$ limit, large fluctuations are observed which, on the average, cancel out. For $\lambda_2{}^{(1)}=-0.4$ polarized regions appear over a broad q range which increase with further decreasing $\lambda_2^{(1)}$. However, close to the zone boundary, the polarization changes sign. This effect becomes more and more localized with further decreasing of the harmonic coupling. In real space (Fig. 4) this effect is very apparent: on a scale of five lattice constants along $\langle 10\rangle$ and $\langle 11\rangle$ the polarization is reversed and then remains the same along both directions (bottom of Fig. 4). Increasing $\lambda_2{}^{(1)}$, the $\langle 10\rangle$ direction remains polarized, but domains appear in the $\langle 11\rangle$ direction. The $\lambda_2{}^{(1)}=0$ case shows strong polarization fluctuations in both directions with incommensurate periodicities. The polarization fluctuations can clearly be related to charge fluc-

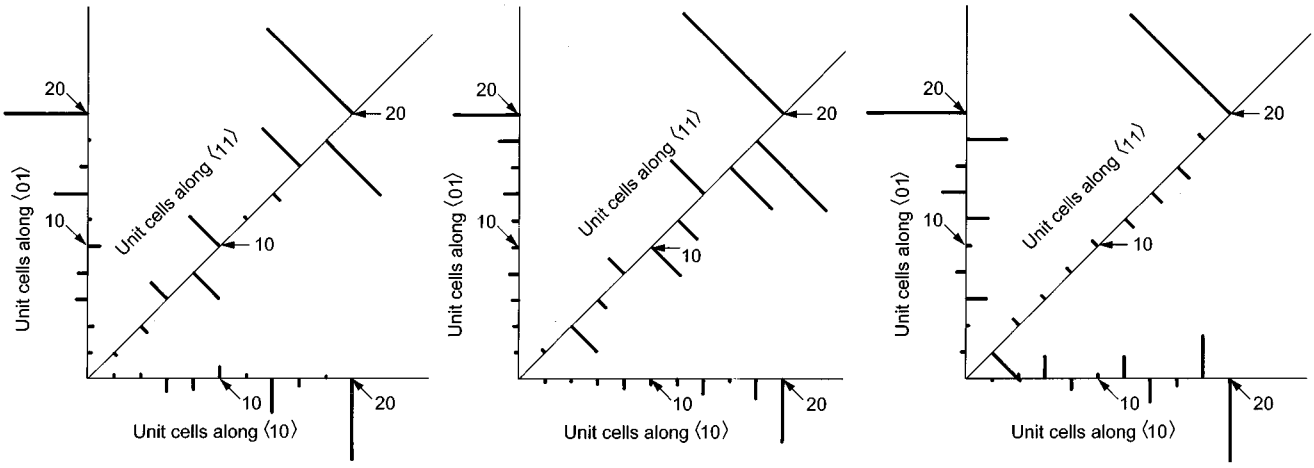

FIG. 5. Real-space displacement of the oxygen ion with $\lambda_2{}^{(1)}$ (from left to right): −0.4, −0.8, −1.2.

tuations in high-temperature superconductors (HTSC's) and the corresponding observed patterns could be triggered by doping as the system becomes more harmonic when approaching the underdoped regime.

We investigate the origin of the above results by looking at the local displacement fields $Q_q^{(1)}$, $Q_q^{(2)}$. We observe that while the transition-metal ion (M_2) displacement is harmonic, i.e., approximately the same in each unit cell, the oxygen ion displacement reflects the various incommensurate, stripe, tweed, and domain patterns which are expected from the effective coupling. In Fig. 5 the local displacement pattern of M_1 is shown for the three cases of $\lambda_2{}^{(1)}<0$. The results discussed above are clarified here in detail. It is obvious from Fig. 5(a) that the structure is incommensurate along $\langle 11\rangle$ and modulated on a scale of six lattice constants along $\langle 10\rangle$. In Fig. 5(b) stripes are formed along $\langle 11\rangle$, while the $\langle 10\rangle$ direction is uniform as expected for harmonic lattices. Figure 5(c) shows the increasing stripe size along $\langle 11\rangle$ now modulated by stripes along $\langle 10\rangle$, i.e., tweed formation. Performing the same calculations along $\langle 21\rangle$ yields a uniform displacement field, i.e., the present results indicate that only the high-symmetry directions are modulated.

In conclusion, we have numerically solved a two-dimensional anharmonic electron-ion interaction model for arbitrary reciprocal-lattice vector, q, which explicitly contains on-site electron-density multiphonon interactions. We find that the effective electron-ion interaction is strongly q dependent due to the higher-order terms and even changes sign for specific q values and $\lambda_2^{(1)}<0$. These sign changes result in local structural instabilities, evidenced as a variety of mesoscale real-space patterns: incommensurate structures, stripe formation, and domain (''tweed'') formation follow with decreasing $\lambda_2^{(1)}$. There are corresponding patterns in the lattice polarization and the local displacement fields. The strong local instability effects which we obtain, are directly attributed to highly anharmonic and aperiodic oxygen ion displacements. The above results suggest that the stripe formation as, e.g., observed in HTSC and colossal magnetoresistance perovskite oxides,[1] depends critically on the depth of local double-well potentials which are driven by the ''polarizability'' effects of electron-density-multiphonon interactions. The discussed model and its solutions can directly be applied to the CuO_2 planes in HTSC's where the suggested patterns have been observed.[1] But similarly it is expected that the chain oxygen ions together with the apex oxygen ion in $YBa_2Cu_3O_7$ act strongly anharmonically and show off-center displacements which do not correspond to the average ideal crystal structure. Specifically the chains could—in analogy to the solutions for the phases—show stripe formations as well as discommensurations. All the above results are complementary to former work on the same Hamiltonian,[6] and as in the earlier work, the electronic degrees of freedom have mainly been addressed, while here emphasis has been put on the lattice degrees of freedom. Both works together thus yield a consistent description of phonon-mediated electron-electron interaction and electron-mediated lattice effects.

The work at Los Alamos was supported by the U.S. D.O.E.

[1] T. Egami, W. Dmowski, T. R. Sendyka, R. S. McQueeney, N. Seigl, H. Yamanchi, Y. Hinatsu, S. Uchida, and M. Arai, in *Proceedings of the International Workshop on Anharmonic Properties of High-T_c Cuprates, Bled, 1994*, edited by D. Mihailovic, G. Ruani, E. Kaldis, and K. A. Müller (World Scientific, Singapore, 1995), p. 118; H. L. Edwards, A. L. Bari, J. T. Makert, and A. L. de Lozanne, Phys. Rev. Lett. **73**, 1154 (1994); S. D. Corradson, J. D. Raistrick, and A. R. Bishop, Science **248**, 1394 (1990); A. Bianconi, in *Proceedings of the International Workshop on Anharmonic Properties of High-T_c Cuprates, Bled, 1994*, edited by D. Mihailovic, G. Ruani, E. Kaldis, and K. A. Müller (World Scientific, Singapore, 1995), p. 125; J. M. Tranquade, B. J. Sternlieb, J. D. Axe, Y. Nakamura, and S. Uchide, Nature (London) **375**, 561 (1995); A. Bianconi, N. L. Saini, A. Lanzara, M. Missori, T. Rossetti, H. Oyanagi, H. Yamaguchi, K. Ota, and T. Ito, Phys. Rev. Lett. **76**, 3412 (1996).

[2] N. Sircon, B. Ravel, Y. Yacobi, E. A. Stern, F. Dogan, and J. J. Rehr, Phys. Rev. B **50**, 13 168 (1994).

[3] A. Bussmann-Holder and A. R. Bishop, Philos. Mag. B **73**, 657 (1996).

[4] A. Bussmann-Holder, A. R. Bishop, and G. Benedek, Phys. Rev. B **53**, 11 521 (1996).

[5] M. Stachiotti, A. Dobry, R. Migoni, and A. Bussmann-Holder, Phys. Rev. B **47**, 2473 (1993).

[6] A. Bussmann-Holder and A. R. Bishop, Phys. Rev. B **44**, 2853 (1991).

[7] R. Migoni H. Bilz, and D. Bäuerle, Phys. Rev. Lett. **37**, 1155 (1976).

[8] Y. Lepine, Phys. Rev. B **28**, 2659 (1983).

[9] S. Kivelson, Phys. Rev. B **28**, 2653 (1983).

[10] E. Pytte, Phys. Rev. B **10**, 4637 (1974); **5**, 3758 (1972); E. Pytte and J. Feder, Phys. Rev. **187**, 1077 (1969).

[11] See, e.g., A. Putnis and E. Salje, Phase Transit. **48**, 85 (1994).